Effect of constant-DI pacing on single cell cardiac dynamics

A THESIS

SUBMITTED TO THE FACULTY OF THE

UNIVERSITY OF MINNESOTA

BY

Preethy Parthiban

IN PARTIAL FULFILLMENT OF THE REQUIERMENTS

FOR THE DEGREE OF

MASTER OF SCIENCE

ADVISOR – Dr. Alena Talkachova

September 2020

Acknowledgements

First and foremost, I would like to thank my advisor, Dr. Alena Talkachova, for giving me my first break in the world of cardiac electrophysiology. I am grateful for the trust and opportunity that she has provided me which has played an integral part in grooming me for graduate school.

I am extremely grateful to my labmates Vasanth Ravikumar, Elizabeth Annoni, Jieun Lee and Xiangzhen Kong for their constant support throughout my program. They stepped in when I had to work remotely and seize an internship which turned out to be a very important career opportunity. Their guidance has played a central role in helping me through mind blocks and seeing my work through to completion. I also thank my committee members Dr. Scott O'Grady and Dr. Taner Akkin for their inputs in finalizing and integrating this document.

Finally, I would like to thank my friends and family back home in India whose support propelled me through all my hard times professionally and personally. Miles apart, their words of encouragement and patient ears got me through many silent struggles. I also extend my thanks to the new circle of trust I gained in Minneapolis who turned the alien dreary winterland into home and held me together as I learned to fall in love with the beautiful land of lakes!

Abstract

Cardiac alternans, beat-to-beat alternations in action potential duration (APD), is a precursor to fatal arrhythmias such as ventricular fibrillation (VF). Previous research has shown that voltage driven alternans can be suppressed by application of constant diastolic interval (DI) pacing protocol. However, the effect of constant-DI pacing on cardiac cell dynamics and its interaction with the intracellular calcium cycle remains to be determined. Therefore, we aimed to examine the effects of constant-DI pacing on the dynamical behavior of isolated cardiac myocytes along with the influence of voltage-calcium (V-Ca) coupling on these changes. Cardiac cell dynamics were analyzed in a non-linear neighborhood close to the bifurcation point using a hybrid pacing protocol, a combination of periodic and constant-DI pacing. We demonstrated that in a small region beneath the bifurcation point constant-DI pacing caused the cardiac cell to remain alternans-free after switching to the constant-BCL pacing, thus introducing a region of bistability (RB). Strong V-Ca coupling increased the size of the RB. Overall, our findings demonstrate that experimental constant-DI pacing on cardiac cells with strong V-Ca strength may induce permanent changes to cardiac cell dynamics increasing the utility of constant-DI pacing.

Table of Contents

List of Tables

List of Figures

CHAPTER 1: INTRODUCTION

1.1 Cardiac Arrhythmias and Heart Failure

Heart failure is the leading cause of death worldwide. In 2017, the American Heart Association reported a total of 17.8 million deaths attributed to cardiovascular diseases (CVD) which was roughly 20% higher than the numbers reported a decade ago (Virani et al., 2020). Apart from the direct impact to heart, cardiac failure contributes to nearly 31% of all deaths by affecting major organ systems such as renal, cerebral, pulmonary and other metabolic pathways. Despite the scientific advancements and pioneering innovation of technology, the socioeconomic burden of heart diseases persists because of lack of understanding molecular-level mechanisms that contribute to the disease progression. Hence, there is a pressing need to elucidate cardiac dynamics at a cellular level.

The average human heart beats 70 times per minute which is more than 36 million times a year and 3 billion times in a lifetime with approximately <1 second resting period between each beat. This feat is achieved by the efficient cardiac conduction system which integrates the electrical and mechanical activity of the heart. A heartbeat begins with the autonomous electrical activity of the pacemaker cells in the sinoatrial (SA) node. This impulse travels down the conduction system via atrioventricular (AV) node, Bundle of His, divides at the bundle branches and terminates at the Purkinje fibers. Consequently, the muscle contraction progresses from atrial contraction which fills up the respective ventricles with blood followed by ventricular contraction which distributes the blood to pulmonary and systemic circulations (Figure.1.1).

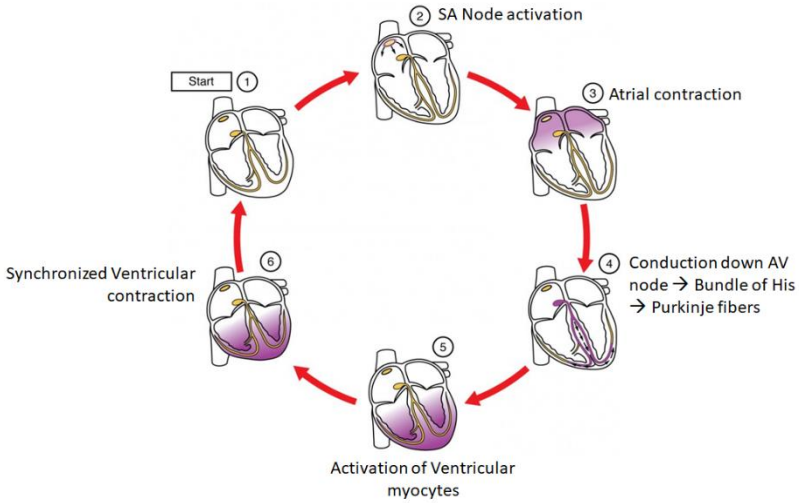

Figure.1.1 Cardiac conduction cycle: Cardiac conduction cycle demonstrating the integration between propagation of electrical activity and mechanical activity in the heart. (*Figure adapted from Lumen Learning – Anatomy and Physiology II)*

Defects in various checkpoints of the conduction-contraction cycle could lead to irregular heart rate or rhythm called *arrhythmia* (Figure 1.2). While some forms of arrhythmia are benign and part of the normal cardiovascular system, persistent arrhythmias impede the heart's ability to pump enough blood required to meet the metabolic needs resulting in fatality. Electrical instabilities eventually lead to death of cardiomyocytes and create obstacles that sustain reentry spiral waves. Table 1.1 summarizes the common forms of arrhythmias classified based on rate (Tachyarrhythmia – pathologically high heart rates vs. Bradyarrhythmia – pathologically slow heart rates) and localization in the heart.

Rate	**Region**	**Arrhythmia**
Tachyarrhythmia	Supraventricular	Atrial Fibrillation

		Atrial Flutter
	Ventricular	Monomorphic ventricular tachycardia
		Polymorphic ventricular tachycardia
		Ventricular Fibrillation
Bradyarrhythmia	Supraventricular	Sinus node dysfunction
	AV Node	Second degree Wenkebach/ Mobitz I block
		Second degree Mobitz II block
		Third degree block
	Ventricular	Ventricular asystole

Table 1.1 Types of Arrhythmias

Arrhythmias are strongly linked to heart failure at the organ level. Depending on the impact of the disease and level of management or care availability heart failure has been classified into 4 stages/classes as shown in Table 1.2.

American College of Cardiology / America Heart Association Stage	**New York Heart Association Class**
A. At risk for heart disease but no actual structural disease	I. No physical limitations
B. Structural disease but no prior or current symptoms of heart failure	II. Slight limitation of physical activity in the form of moderate exertion
C. Structural disease with past or current symptoms of heart failure	III. Marked limitation of physical activity in the form of minimal exertion

D. End-stage disease (does not respond satisfactory to treatment)	IV. Inability to exert because of symptoms of heart failure at rest

Table 1.2 Classification of heart failure

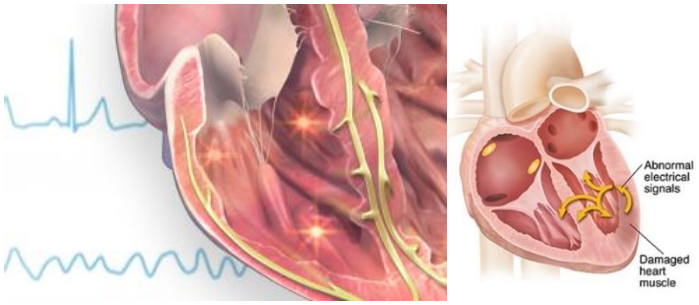

Figure 1.2 Electrical instabilities and cardiac arrhythmias: Abnormal electrical signals in the heart could lead to obstacles impeding the normal propagation of electrical activity and result in arrhythmias.

1.2 Cardiac Interventions – The Pacemaker

Irrespective of the origin and state of heart failure, arrhythmias persist to be reliable mechanism for sustenance of diseased states. Hence, various cardiac interventions have been developed to treat and prevent arrhythmias. The history of pacemakers – devices that provide an external electrical stimulus to create or modify existing irregularities in cardiac mechanical activity – is vast and rich. The first instance of pacemaker dates to 1930s with Hyman's '*artificial pacemaker'* which was a bulky AC-powered device with an extension cord and terminal leads that stimulated the myocardium intercostally. Since then, various advancements in the field have led to more elegant and minimally invasive

versions of pacemakers. A significant milestone in this journey is attributed to Dr. C. Walton Lillehei and Earl Bakken from University of Minnesota for inventing the first battery-powered pacemaker (Mulpuru, Madhavan, McLeod, Cha, & Friedman, 2017). Currently, the future of pacemakers is headed towards a model of self-powered device integrating piezoelectric nanogenerators that utilize the electrical energy generated from body movements.

Figure 1.3 Self-powered cardiac pacemaker: First demonstration of a self-powered cardiac pacemaker by The Korea Advanced Institute of Science and Technology (KAIST)

1.3 Prediction of Arrhythmias

The basic function of pacemaker entails efficient prediction of arrhythmias and generation of an appropriate impulse to mitigate the onset. However, this task is complicated by the complex spatiotemporal heterogeneities of the heart. A well-known precursor to cardiac arrhythmias at the cellular level is alternans.

Cardiac alternans is often considered to be a precursor to tachycardia, fibrillation and other dangerous heart arrhythmias (Narayan, 2006; Verrier & Malik, 2013; Walker & Rosenbaum, 2003a). Thus, many strategies to eliminate alternans have been developed. Specifically, delayed feedback control was proposed to control periodic systems, such as in human patients with pacing induced period-2 atrioventricular-nodal conduction alternans, or small pieces of in-vitro paced bullfrog myocardium with APD alternans (Zlochiver, Johnson, & Tolkacheva, 2017). Delayed feedback control often applies various modifications to periodic stimulation, otherwise known as constant-BCL pacing. When cardiac cell is paced periodically, with constant basic cycle length (BCL), each stimulus produces an action potential and the following relationship is valid:

$$BCL = APD_n + DI_n \tag{1}$$

where BCL is basic cycle length (BCL), APD_n and DI_n are action potential duration and diastolic interval following nth stimuli (see Figure 1.4).

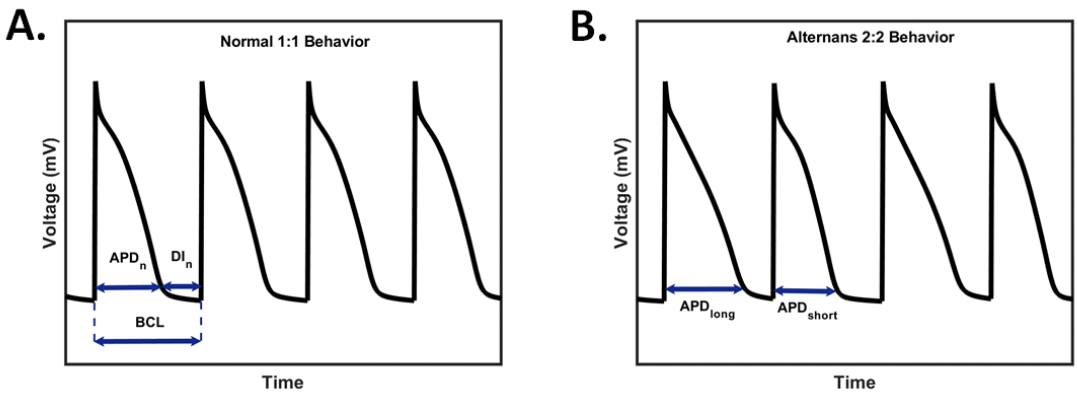

Figure 1.4 Alternans vs. normal cardiac rhythm: A) Normal 1:1 response and B) alternans during periodic acing (Eq. 1).

Recently, we and others proposed and demonstrated the effectiveness of constant-DI pacing to eliminate alternans and establish stable 1:1 rhythms in single-cell, one-dimensional and two-dimensional models (Cherry, 2017; Jordan & Christini, 2004a; Zlochiver et al., 2017). Constant-DI pacing works on the principle of maintaining a predetermined diastolic interval which would then influence and maintain a constant action potential duration. However, the success was spatially limited to regions close to the pacing electrode. Simultaneous studies have attributed the onset of alternans to ionic mechanisms. One of the hypotheses states that at rapid heart rates the capacity of cardiac cells to cycle intracellular Ca^{+2} is exceeded. A cascade of abnormal electrogenic Ca^{2+}-sensitive currents could then cause APD alternans (Cherry, 2017; Hayashi et al., 2007; Kihara & Morgan, 1991; McIntyre, Mori, & Tolkacheva, 2011).

Although many studies have elucidated the potential and drawbacks of constant-DI pacing in mathematical models, there has been no in-depth study of the cellular impact of

constant-DI pacing. Particularly the link between constant-DI pacing and intracellular calcium dynamics is not well established. In this study we aimed to determine the effect of constant DI pacing on dynamical behavior of cardiac cell. We also attempt to investigate the importance of V-Ca coupling strength on the alternans formation in cardiac cell Specifically, we aim to determine whether constant-DI pacing changes the cardiac cell dynamics close to the bifurcation point when subject to voltage-driven alternans and analyze the sensitivity of the induced changes to V-Ca coupling strength.

Road map:

CHAPTER 2: Literature Review

In this chapter the reader will be introduced to an in-depth discussion of alternans and their contribution to progression of heart diseases. Further, the reader will be acquainted with important concepts of cardiac dynamics and voltage-calcium relationship in the heart. The chapter will conclude with a detailed discussion of pacing interventions – types, advantages and disadvantages – developed to prevent alternans formation.

CHAPTER 3: Methodology

In Chapter 3, the details of the mathematical model used, and experimental approaches will be presented. It will provide elaboration of how constant-DI pacing was implemented *in silico* and introduce the hybrid pacing model utilized to study the response of the cardiac cell.

CHAPTER 4: Results and Discussion

In Chapter 4, the main observations in response to the distinct pacing protocols will be presented. The novel behavior of cell in response to constant-DI pacing will be introduced

with discussion on how these results could be utilized to improve the benefits of constant-DI pacing.

CHAPTER 5: Conclusion

This chapter summarizes the central hypothesis, technical approach and main results of this study. The novelties and limitations specific to this study will be emphasized. The chapter will conclude with recommendations for the future scope of this work.

CHAPTER 2: LITERATURE REVIEW

2.1 History of Alternans and Clinical Relevance

The earliest reports of alternans dates to early 20th century when H. E. Hering (Walker & Rosenbaum, 2003a) first reported the occurrence of ECG alternans in an animal model following the administration of glycolytic acid. Two years later, Sir Thomas Lewis (Walker & Rosenbaum, 2003a) made a similar observation that led him to hypothesize the crux of alternans and its relevance as a predictor of cardiac arrhythmias – "*alternation occurs either when the heart muscle is normal and the heart rate is very fast, or when there is serious cardiac disease and the rate is normal*". Moreover, the multitude of studies reporting the occurrence of ECG alternans establish it as a global marker of arrhythmias independent of the underlying cause (Kanu, Iravanian, Gilmour, & Christini, n.d.; Verrier & Malik, 2013).

In various animal models and human subjects, it has been observed that occurrence of cellular alternans can be closely linked to higher propensity of developing cardiac arrhythmias. Prior studies have established a close association between alternans at the level of myocytes and manifestation of ventricular T-wave alternans (TWA). TWA or beat-to-beat alternation in the amplitude of T-waves has been identified as a clinical predictor of ventricular arrhythmias like ventricular fibrillation (VF) and even sudden cardiac death (SCD) (Pastore, Girouard, Laurita, Akar, & Rosenbaum, 1999).

2.2 Factors contributing to Alternans

2.2.1 Restitution

Restitution describes the relationship between action potential duration (APD) and the preceding diastolic interval (DI) in the heart.

The dynamics of cardiac cell are usually described by a restitution relation:

$$APD_{n+1} = R_c(DI_n) \quad (2)$$

which provides the dependence of the subsequent APD_{n+1} on preceding DI_n and the function R_c defines the restitution curve between APD and DI. At physiological heart rates, this phenomenon is integral for APD adaptation and maintenance of a stable rhythm. However, at higher heart rates restitution eventually leads to alternans progressing into a rhythm of short DI causing a short APD leading to subsequent long DI causing a long APD. Graphically, this relationship is interpreted through the restitution curve which plots APD as a function of preceding DI (Figure 2.1). A steep restitution curve would mean that small changes in DI could lead to large fluctuations in APD.

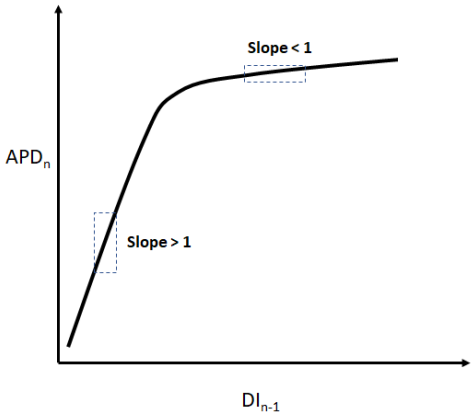

Figure 2.1 Restitution Curve: A steep Rc function with slope > 1 could indicate large fluctuations in APD due to small changes in DI leading to alternans. A shallow Rc function with slope < 1 is hypothesized to suppress alternans and lead to a normal rhythm.

Experimentally, several groups claimed that unstable alternans are caused when the slope of restitution curve exceeds 1. Hence, the 'Restitution Hypothesis' was formed based on the feedback relationship between APD and DI, claiming that flattening the slope of restitution curve could prevent alternans by eventually suppressing the alternating rhythm.

This theory has had modest success since some drugs aimed at flattening the curve have successfully eliminated alternans (Bauer, Röder, & Bär, 2007; Cram, Rao, & Tolkacheva, 2011). However, it is limited by a few drawbacks. The restitution curve does not capture the complex dynamics of various ion channels that contribute towards the development of alternans. This limits its capability to provide any useful insight on the origin of alternans. Furthermore, the restitution hypothesis fails to hold true in cases like severe ischemia, where alternans persist despite a shallow restitution curve. Another integral component of cardiac dynamics involves heart rate variability (HRV) (McIntyre, Kakade, Mori, & Tolkacheva, 2014). The normal cardiac rhythm is prone to subtle fluctuations on a beat-to-beat basis. Pacing strategies solely aimed at restitution hypothesis fail to capture the temporal complexity of HRV. However, the existence of feedback between APD and DI indicates that appropriate manipulation of DI will consequently affect APD and could be exploited to revert alternans.

2.2.2 Intracellular Calcium cycle

Deriving from the restitution hypothesis one would expect constant-DI pacing to eliminate alternans. In this regard, various groups including ourselves have shown significant success in eliminating alternans in single-cell, one-dimensional cable and two-dimensional cardiac models using constant-DI pacing (Cherry, 2017; Jordan & Christini,

2004a; Kulkarni, Lee, Kluck, & Tolkacheva, 2018; Zlochiver et al., 2017). However, the rate of success declines with the increase in complexity of structure, pacing parameters and ionic mechanisms defined in the *in silico* model. These results indicate that there are distinct restitution-independent mechanisms that drive alternans.

Parallel investigation of mechanical alternans has brought to light the important contributions of intracellular calcium cycling and its effects on APD alternans. Henceforth, alternans has been divided into two broad categories: voltage-driven alternans originating due to instabilities in transmembrane voltage and calcium-driven alternans originating due to dysregulated intracellular calcium cycle. A possible explanation for the failure of constant-DI pacing models was that the alternans, in such cases, was driven by a different mechanism such as the calcium cycle which does not depend on the restitution feedback. A comprehensive study by E.M.Cherry (Cherry, 2017) dissected the varying types of alternans and the specific contribution of constant-DI pacing in eliminating each type. This study concluded that constant-DI pacing is effective in eliminating V-driven alternans while it fails to suppress Ca-driven alternans (Refer Figure 4.1). However, the cellular mechanisms that mediate these effects of constant-DI pacing remain elusive.

2.2.3 Other factors

Periodically paced cardiomyocytes can retain parametric dynamics that depend on their pacing history. This ability is termed *short-term memory* impeding the cardiac dynamics to be described by a single restitution function since the changes to APD are not limited to preceding DI but depend on the entire pacing history (Cherry & Fenton, 2004).

Spatially alternans can be classified as concordant or discordant. While concordant alternans could be benign, discordant alternans – displaying out-of-phase APD

alternations in neighboring regions of the heart are proarrhythmogenic. Discordant alternans lead to reentry wave patterns causing spatial heterogeneity in repolarization (Watanabe, Fenton, Evans, Hastings, & Karma, 2001).

2.3 Voltage-Calcium coupling – The role of sodium-calcium exchanger

As discussed in the introduction (Figure 1.1), the electrical system of the heart is closely associated with the mechanical contraction system. Hence, it comes as no surprise that the intracellular calcium cycle plays an important role in regulating the voltage dynamics. These impacts are driven by the Excitation-Contraction coupling system in the heart. At the cellular level, when a cardiomyocyte is excited with an electrical impulse, the activation (or depolarization) is caused by a flood of sodium ions entering the cell. The depolarization wave flows down along invaginations called T-tubules and open voltage-gated calcium channels on their membrane. This causes modest release of calcium ions into the cytoplasm which in turn opens calcium channels on the sarcoplasmic reticulum which constitutes the intracellular calcium storage in all myocytes, leading to a significant (~100 fold) increase in intercellular calcium concentration. This spike in calcium ions leads to downstream activation of the contractile mechanisms in the heart (Troponin-complex mediated muscle contraction). Effective removal of calcium from the intercellular space dictates appropriate muscle relaxation. Important channels involved in this process include sodium-calcium exchanger (NCX), Plasma-membrane Calcium ATPase and sarcoplasmic-endoplasmic reticulum calcium ATPase (SERCA) pump. While NCX extrudes the calcium into extracellular space, SERCA pumps facilitate reuptake of calcium into SR stores. The balance between these two mechanisms decides the availability of SR calcium for the following heartbeat. In large mammals, the sodium calcium exchanger located on the plasma membrane is a major contributor to calcium extrusion from the cell.

A dominant NCX action could leave the SR depleted with insufficient Ca^{2+} to produce force, while weak extrusion by NCX could lead to overload of calcium causing insufficient relaxation and eventual cell death.

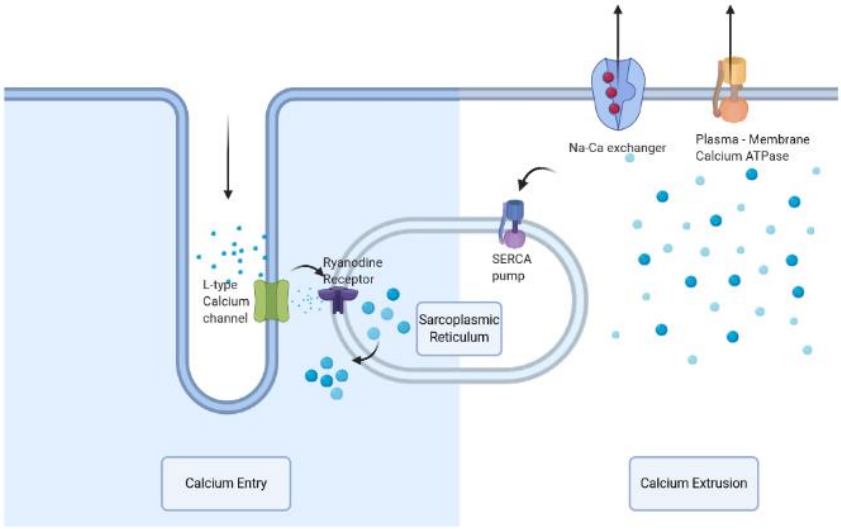

Figure 2.2 Intracellular calcium cycle: Calcium Entry – L-type calcium channels allow entry of extracellular calcium into the cytoplasm; Ryanodine Receptors sense cytoplasmic calcium and lead to elevated calcium release from the sarcoplasmic reticulum. Calcium Extrusion – SERCA pumps allow calcium reuptake from the cytoplasm and enable relaxation; Sodium calcium exchanger and Plasma-membrane calcium ATPase allow extrusion of calcium into the extracellular space.

The NCX functions by transporting 3 sodium molecules in exchange for 1 calcium molecule making it an electrogenic transporter which could potentially affect membrane voltage and excitability of the cardiomyocyte. It functions in two modes of action depending

on the concentration gradient of the Na^+ and Ca^{2+} ions, and the corresponding driving force for the exchanger. In forward mode, sodium is taken into the cell in exchange for calcium extruded from the cell. In the reverse mode, implicated in pathophysiological arrhythmogenic conditions, the exchanger can extrude sodium and uptake calcium into the cell. The strength of the exchanger in either direction (or mode of action) is determined by the value of its conductance (g_{NaCa}). Chapter 4.3 presents in-depth discussion on specific effects of coupling strength of voltage and calcium dynamics under steady state conditions with and without alternans.

2.4 Paced Cardiomyocyte – Anti-alternans pacing protocols

Cardiac cells are excitable cells and readily respond to external electrical stimuli. This has laid the foundation to pacing protocols designed for control and elimination of alternans. If the cardiac cell described by Eq. 3 is being paced periodically (Eq. 1), normal rhythm (1:1) (see Figure.1.4 A) becomes unstable and transfers to alternans (2:2) (see Figure.1.4 B), with alternating long and short APD intervals (APD_{long} and APD_{short}), when the slope of the restitution curve $R_c = 1$. Initial approaches to suppress alternans pursued the traditional route of eliminating the restitution feedback described in Eq. 2. based on modification of Eq. 1 (Christini et al., 2006; Kanu et al., n.d.)

However, as discussed earlier subsequent studies disproved the necessity of the restitution hypothesis to maintain alternans depending on the mechanism of alternans formation. In this section we will discuss the motivation behind classical pacing protocols used for eliminating alternans and proceed to introduce constant-DI pacing to address the drawbacks with the conventional approaches.

Constant BCL pacing:

The earliest effort to suppress alternans was the introduction of constant-BCL (basic cycle length) or periodic pacing in the heart. This protocol is founded based on restitution hypothesis. It was believed that maintaining a constant pacing period would force temporally local adaptations of APD and stabilize a normal 1:1 rhythm. However, this approach was lacking due to various factors (such as HRV, spatial heterogeneity, conduction velocity, short-term memory, intra-cellular calcium dynamics) that have been discussed in previous sections. Further, on an implementational level, constant-BCL pacing required a comprehensive knowledge of the unstable dynamics ahead of designing the pacing strategy. This was cumbersome for a clinical solution. The failure of constant-BCL pacing encouraged the exploration of pacing protocols that could integrate the spatio-temporal heterogeneities in the heart and allow clinical implementation with minimal prior knowledge of the cardiac dynamics.

Delayed feedback control:

An attractive solution to the clinical manifestation of constant-BCL pacing was provided by the Delayed Feedback Control (DFC) approach. This method employed a dynamic system that updated the pacing interval required to maintain a constant BCL by constantly updating a gain parameter that suppressed the difference between the last two APDs. Since the algorithm depended only on the last two APDs, real-time application of this approach was feasible. However, DFC failed to control alternans that were distal from the pacing electrode and its success was limited to small-scale systems (Echebarria & Karma, 2002).

Adaptive DI pacing:

The drawbacks of constant-BCL pacing were overcome by removing the feedback between APD and DI. In 2004, Jordan and Christini proposed the Adaptive DI pacing method which employed dynamically updating the DI by adjusting a control parameter that influenced the difference between the target BCL and BCL of the last pulse. Despite the motivation to eliminate restitution-dependent alternans, this strategy indirectly incorporated the feedback between APD and DI. Further, the model used was an outdated and inaccurate description of relevant clinical models. Hence, the application of adaptive-DI pacing was not beneficial in comparison to DFC (Jordan & Christini, 2004b).

Constant-DI pacing:

Integrating the results from these approaches we have validated the use of a constant-DI pacing protocol to suppress alternans both *in silico* (Zlochiver et al., 2017) and *ex vivo* (Kulkarni et al., 2018). In this approach we eliminate the dependency between APD and preceding DI by applying a stimulus at the end of a precomputed fixed DI interval. *In silico*, we verified that this approach was successful in suppressing, at least, restitution-dependent alternans. As introduced earlier, a study by E.M.Cherry concluded that constant-DI pacing was successful in suppressing V-dependent alternans while it failed to suppress Ca-driven alternans. As an extension to this concept, our laboratory implemented a version of constant-DI pacing in *ex vivo* rabbit hearts by applying a stimulus after precalculated constant TR-interval measured in real-time using a volume conducted 3-electrode ECG. The results of this study indicated that the real-time constant TR pacing could flatten the slope of the restitution curve and indicate that there are anti-arrhythmic benefits to this approach. However, an accurate implementation of real-time constant-DI pacing in *ex vivo* hearts remains to be challenging.

CHAPTER 3: MATERIALS AND METHODS

3.1. Mathematical Model

A Mahajan-Shiferaw rabbit ventricular single-cell model (Mahajan et al., 2008) was chosen for its well-described intracellular Ca^{2+} cycle (Shiferaw, Watanabe, Garfinkel, Weiss, & Karma, 2003) at rapid heart rates using a Markovian scheme. The sodium-calcium exchange current is designed following Shannon and Hund-Rudy equations with a sodium-calcium exchanger conductance parameter (g_{NaCa}) that controls the activity of the exchanger. The g_{NaCa} was adjusted to alter the V-Ca coupling strength as shown in Table I. The relation between the exchanger current (I_{NCX}) and gNaCa is illustrated in the Appendix. The slope of the sarcoplasmic reticulum (SR) calcium release function (u) was used to provide either V-driven (u = 9.5 s^{-1}) or Ca-driven (u = 11.3 s^{-1}) alternans, as described in (Mahajan et al., 2008; Shiferaw et al., 2003).

V-Ca Coupling Strength	Extra Strong	Strong	Normal	Weak
g_{NaCa} (uM/s)	0.75	0.8	0.84	0.88

Table 3.1 The sodium-calcium exchanger conductance (g_{NaCa}) for each V-Ca coupling strength (Mahajan et al., 2008)

3.2. Pacing Protocol

In order to investigate whether constant-DI pacing altered the dynamical behavior of the paced cardiac cell, we implemented a hybrid pacing protocol consisting of three sequences. In each of the following sequences, 5000 stimuli pulses were applied to allow the system to reach a steady state:

1) First, constant-BCL pacing with BCL = BCL_1 was applied to the cell following Eq. 1. A wide range down sweep protocol was utilized to find the range of BCLs close to bifurcation. For this the cell was paced from BCL = 400 ms to 100 ms with a progressive decrease in steps of 10 ms. After narrowing down to the region close to bifurcation, the value of BCL_1 started at 220 ms and was progressively decreased to 205 ms in steps of 1 ms (see Figure 2A, red arrows). Steady state APD and DI (APD_{SS} and DI_{SS}) were recorded as the average taken from the last 10 pacing cycles.

(2) Then constant-DI pacing was applied (see Figure 2B, red arrows). The end of each APD was measured in real time, and stimuli were applied after waiting for a predetermined interval, DI_{const}, which was calculated based on the previous constant-BCL pacing values:

$$DI_{const} = BCL_1 - APD_{SS} \quad (3)$$

The equivalent BCL (BCL_{eq}) was computed at the end of constant-DI pacing to facilitate the comparison between the constant-DI sequence and the constant BCL sequence.

$$BCL_{eq} = DI_{const} + APD \quad (4)$$

where, APD is the average duration of last 10 action potentials paced with DI_{const}.

(3) Thirdly, to evaluate the changes to the dynamical behavior caused by constant-DI pacing, 100 stimuli pulses were applied immediately after the constant-DI sequence at

$$BCL_2 = BCL_1 + \delta \quad (5)$$

where δ = 0 (i.e. $BCL_2 = BCL_1$) for hybrid pacing without perturbation (see Figure 2C) and δ = [-10, 10] ms varied in steps of 1 ms, for the hybrid pacing protocol with perturbation (see Figure 2D). The perturbation was expected to deviate the changes induced by constant-DI pacing and hence provide a quantifiable measure of its robustness.

(4) Finally, constant-BCL pacing at $BCL = BCL_1$ was applied to return the system to a steady state.

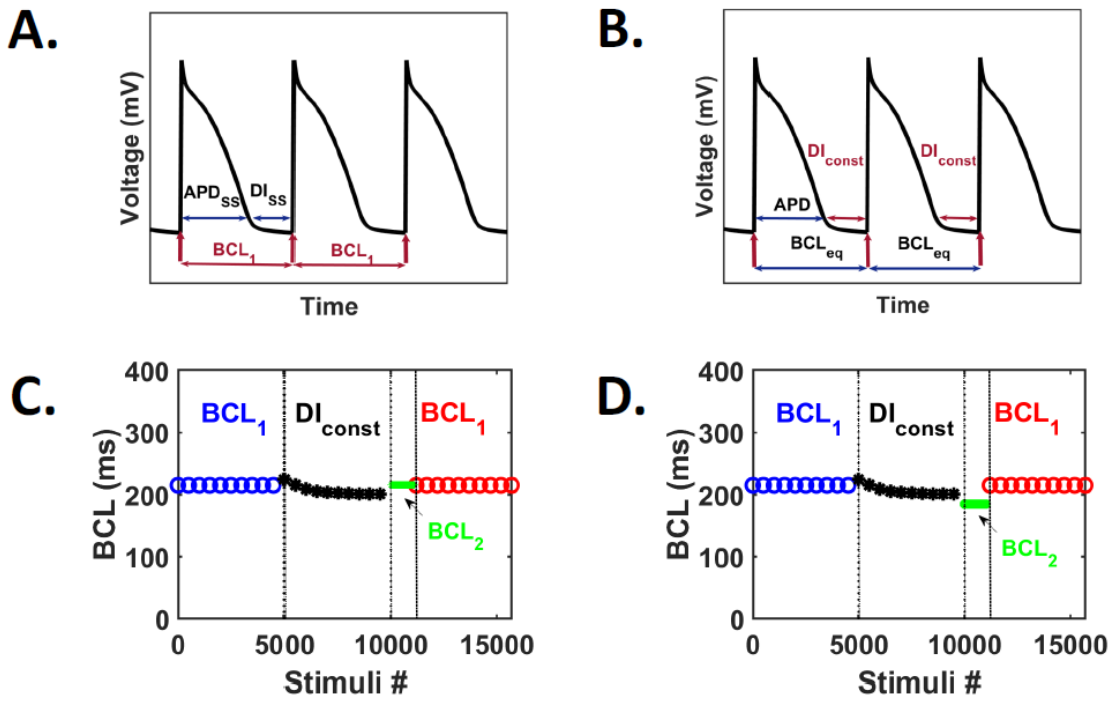

Figure 3.1 Pacing strategies: A) Constant-BCL pacing: stimuli (red arrow) are applied at a predetermined BCL_1 (see Eq. 1). B) Constant-DI pacing: stimuli (red arrow) are applied at the end of predetermined DI_{const} (see Eq. 2). C) Hybrid pacing without perturbation: 5000 stimuli are applied in at BCL_1 (blue) and DI_{const} (black); then 100 stimuli are applied at $BCL_2 = BCL_1$ (green), i.e. d = 0 ms in Eq. 4; finally 4900 stimuli are applied at BCL_1 (red). D)

Hybrid pacing with perturbation: Like C), but $BCL_2 = BCL_1 - 10$ ms (green), i.e. d = -10 ms in Eq. 4.

3.3. Analysis

At the end of each pacing sequence, steady state APD_{SS} was calculated at the 80% repolarization level. Bifurcation diagrams were constructed by plotting APD_{SS} as a function of BCL (during periodic pacing) or BCL_{eq} (during constant-DI pacing). During alternans, APD_{long} and APD_{short} (see Figure 1B) were calculated as the respective means of odd and even beats from last 10 steady state responses. The magnitude of alternans was computed as follows:

$$\Delta APD_a = |APD_{long} - APD_{short}| \quad (6)$$

and a ΔAPD_a = 5 ms was set as the alternans threshold. The onset of alternans was defined as the smallest value of BCL (BCL_{onset}) that resulted in a 1:1 response before the transition into alternans.

CHAPTER 4: RESULTS AND DISCUSSION

4.1 Constant-DI pacing suppresses voltage-driven alternans:

The cardiac cell with either V-driven and Ca-driven alternans was paced using constant-BCL and constant-DI protocols, and corresponding bifurcation diagrams were then constructed. As expected, constant-BCL pacing resulted in the formation of alternans both V-driven (Figure 4.1 A, BCL_{onset} = 213.5 ms) and Ca-driven (Figure 4.1 C, BCL_{onset} = 241 ms). The application of constant-DI pacing only suppressed V-driven but not Ca-driven alternans (Figure 4.1 B and 4.1 D), in agreement with previous studies (Cherry, 2017; Zlochiver et al., 2017). Nevertheless, constant-DI pacing resulted in lowering the BCL_{onset} for Ca-driven alternans, from 241 ms to 223 ms.

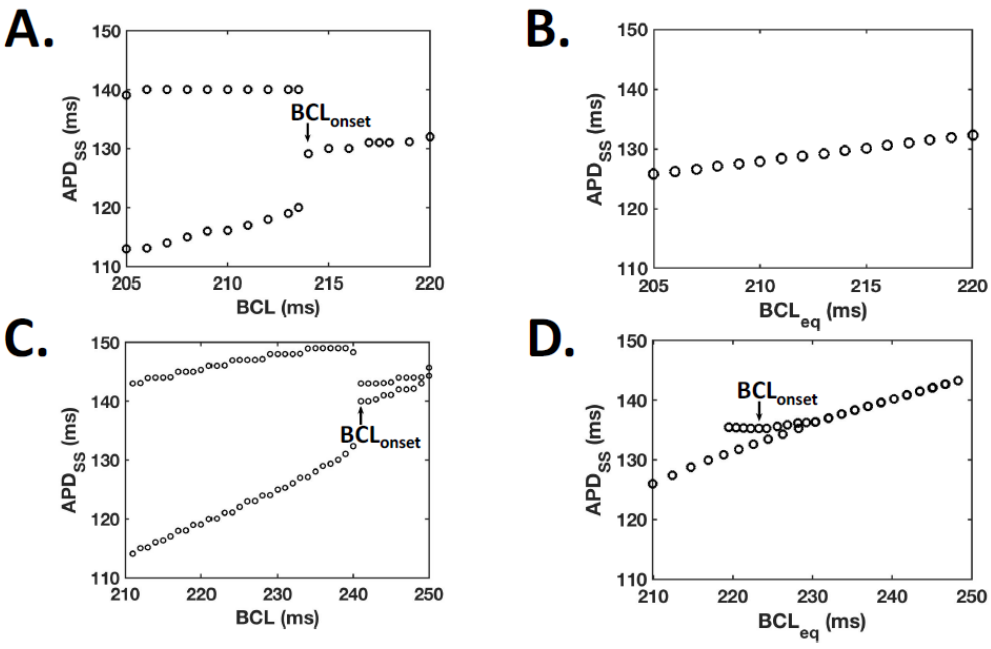

Figure 4.1 Ability of constant-DI pacing to suppress V-driven compared to Ca-driven alternans: Bifurcation diagrams constructed with normal V-Ca coupling for constant-BCL

(A, C) or constant-DI (B, D) pacing in the case of V-driven (A, B) and Ca-driven (C, D) alternans configuration. Arrows indicate the onset of alternans BCL_{onset} = 213.5 ms (A), 241 ms (C) and 223 ms (D). No alternans is present in (B).

4.2 Constant-DI pacing introduces a region of bistability (RB):

In order to investigate the effect of constant-DI pacing on the dynamic responses of the cardiac cell, we applied the hybrid pacing protocol without perturbation ($BCL_1 \rightarrow DI_{const} \rightarrow BCL_1$) to it. Figure 4.2 A shows the two overlapping bifurcation diagrams: before (blue) and after (red) application of constant-DI pacing. Note that application of constant-DI pacing shifted BCL_{onset} to a lower value (see Figure 4.2 A). Three different regions for constant-BCL pacing following constant-DI pacing were identified based on proximity to the BCL_{onset} prior to constant-DI pacing (marked in Figure 4.2 A):

(1) region 1, where $BCL_1 << BCL_{onset}$,

(2) region 2, where $BCL_1 \sim BCL_{onset}$

(3) region 3, where $BCL_1 >> BCL_{onset}$.

Representative values for BCL_1 were chosen from each region - 1) BCL_1 = 208 ms, 2) BCL_1 = 213.5 ms and 3) BCL_1 = 219 ms. The responses of the cell to hybrid pacing are shown in Figure 4B for the three different regions. When $BCL_1 << BCL_{onset}$ the cardiac cell exhibits alternans at the end of the first constant-BCL segment. Alternans is suppressed when constant-DI pacing is applied but reappears upon application of the second constant-BCL segment.

When BCL_1 ~ BCL_{onset}, the alternans at the end of the first constant-BCL segment is suppressed by applying constant-DI pacing, and subsequent constant-BCL pacing fails to initiate it. Such behavior suggests that the system has a region of bistability (RB) between alternans and a 1:1 response during constant-BCL pacing, and that constant-DI pacing acts as a trigger to switch between the two states.

For the BCL_1 >> BCL_{onset} the system exhibits a stable 1:1 response independent of the pacing sequence. Therefore, our results indicate that the presence of constant-DI pacing affects the dynamics of cardiac cells in an anti-alternans manner.

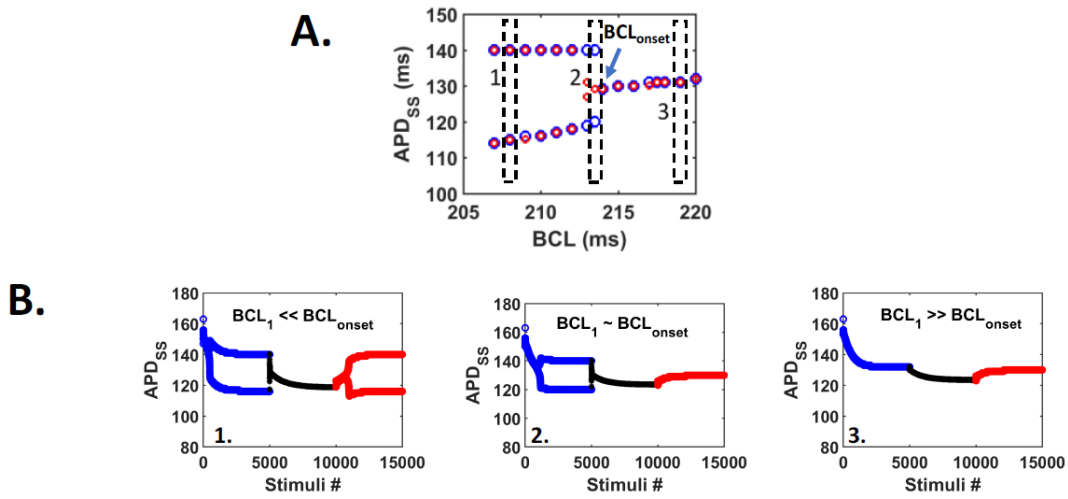

Figure 4.2 Hybrid pacing uncovers Region of bistability: A) Overlap of bifurcation diagrams from hybrid pacing: constant-BCL pacing at BCL_1 before (blue) and after (red) constant-DI pacing. Note the formation of alternans at BCL_{onset} = 213.5 ms for constant-BCL pacing before, but not after constant-DI pacing (shifted lower to 212 ms). B) Responses of the cardiac cell to hybrid pacing at three regions that were chosen in (A)

depending on the value of BCL_1 with respect to BCL_{onset}: (1) $BCL_1 << BCL_{onset}$; (2) $BCL_1 \sim BCL_{onset}$; (3) $BCL_1 >> BCL_{onset}$

Region	Constant BCL_1	Constant DI	Constant BCL_1
$BCL_1 << BCL_{onset}$	2:2	1:1	2:2
$BCL_1 \sim BCL_{onset}$	2:2	1:1	1:1
$BCL_1 >> BCL_{onset}$	1:1	1:1	1:1

Table 4.1 Dynamical response of the cardiac cell for different regions (*as identified in Figure 4.2*)

4.3 Effect of coupling-strength:

Next, we sought to investigate the effect of V-Ca coupling strength on BCL_{onset}. The overlapping bifurcation diagrams for the down-sweep constant-BCL protocol with weak (green), normal (blue) and strong (red) V-Ca coupling (see Table 3. 1) are shown in Figure 4.3. Note that increasing (decreasing) the V-Ca coupling strength decreased (increased) BCL_{onset} to 211 ms (218 ms) from the normal value of BCL_{onset} = 213.5 ms.

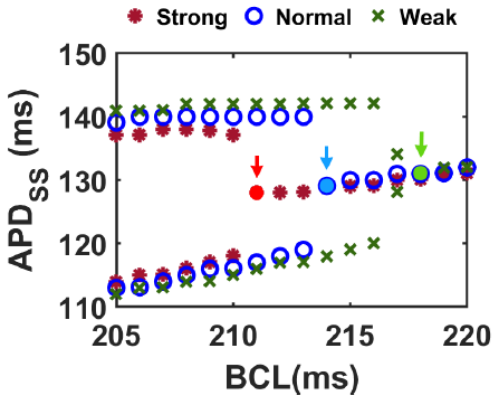

Figure 4.3 Effect of coupling strength on onset of alternans: The effect of V-Ca coupling strength (see Table 3.1) on bifurcation diagram of cardiac cell under constant-BCL pacing. The BCL_{onset} (arrows) shift to lower values of BCL as V-Ca coupling strength increases from weak (BCL_{onset} = 218 ms) to normal (BCL_{onset} = 213.5 ms) to strong (BCL_{onset} = 211 ms) V-Ca coupling.

We then investigated the effect of coupling strength on the voltage and calcium dynamics under steady state in both no-alternans and alternans conditions. We paced the cell at a BCL > BCL_{onset} to emulate steady state without alternans for various coupling strengths (g_{NaCa} ranging from 0.1 to 1 uM/s). The corresponding APD and height of calcium-transient is depicted in Figure 4.4. Representative voltage and Ca-transient traces for three coupling strengths are attached in the Appendix (Figure A.2). It can be seen the APD for a given BCL decreases with increase in coupling strength, while the amplitude of calcium-transient increases - indicating greater capability for APD adaptation with stronger calcium dynamics at higher coupling strengths.

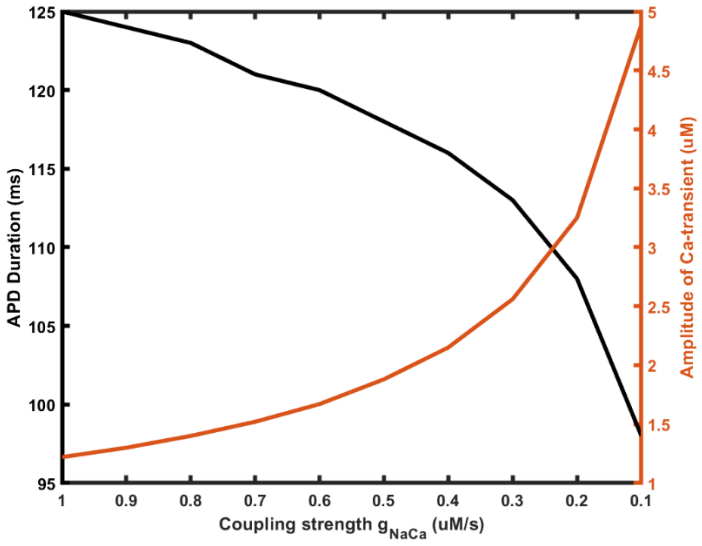

Figure 4.4 Effect of coupling strength on APD duration and amplitude of calcium-transient under steady-state condition without alternans The cell was paced at a constant BCL = 230 ms (no alternans condition) with varying coupling strengths and the duration of APD and amplitude of Ca-transient was plotted with increasing coupling strength (or decrease in g_{NaCa} values)

Next, we investigated the voltage and calcium dynamics in the presence of alternans. For this, we paced the cell at three representative coupling strengths (Weak, Normal and Strong) as discussed previously. We paced the cell at a constant BCL = BCL_{onset} – 10 ms to emulate a standard region of alternans across various coupling strengths. The corresponding amplitude of APD and calcium-alternans is summarized in Table 4.2. The APD alternans decrease with an increase in coupling strength, while the calcium-alternans increase with increasing coupling strength.

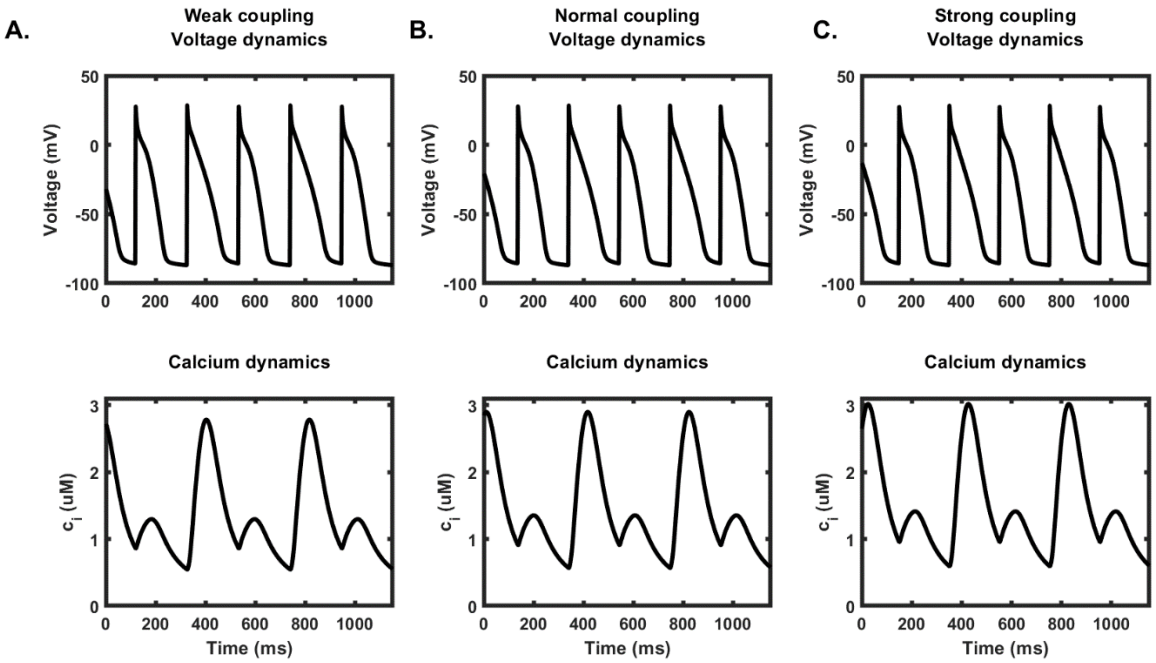

Figure 4.5 Changes in voltage and calcium dynamics with coupling strength (alternans rhythm) The rabbit cell was paced at a constant $BCL_1 = BCL_{onset} - 10$ ms (alternans region) and the corresponding V-alternans and calcium-alternans amplitude was compared between the different coupling strengths. A) Weak coupling (BCL_1 = 207 ms) B) Normal coupling (BCL_1 = 203.5 ms) C) Strong coupling (BCL_1 = 201 ms). The amplitude of APD and calcium alternans are summarized in Table. 4.2

Coupling strength	**Weak**	**Normal**	**Strong**
Amplitude of APD-alternans (ms)	25	23	22

Amplitude of calcium-alternans (uM)	1.49	1.55	1.61

Table 4.2 APD and calcium alternans with varying coupling strengths

We then applied hybrid pacing without perturbation ($BCL_1 \rightarrow DI_{const} \rightarrow BCL_1$) at varying levels of V-Ca coupling strengths (see Table 3.1). Figure 4.6 A and 4.6 B show the change in the bifurcation diagrams obtained during constant-BCL pacing before (blue) and after (red) constant-DI pacing for strong and weak V-Ca coupling, respectively. Note the presence of a RB = 3 ms for strong V-Ca coupling, due to the different values of BCL_{onset} before and after constant-DI pacing. This is not the case for weak V-Ca coupling, where no RB is observed (see Figure 4.6 B). Figure 4.6 C compares RBs for different V-Ca coupling strengths. Note that the RB increases with increasing V-Ca coupling strength. Figure 4.6 D demonstrates the relative shift in BCL_{onset} as a function of V-Ca coupling strength. As the V-Ca coupling strength increases, the difference between BCL_{onset} before and after application of constant-DI protocol increases, thus increasing RB. Overall, this suggests that increasing V-Ca coupling strength facilitates changes in the cell dynamics that are triggered by the application of constant-DI pacing.

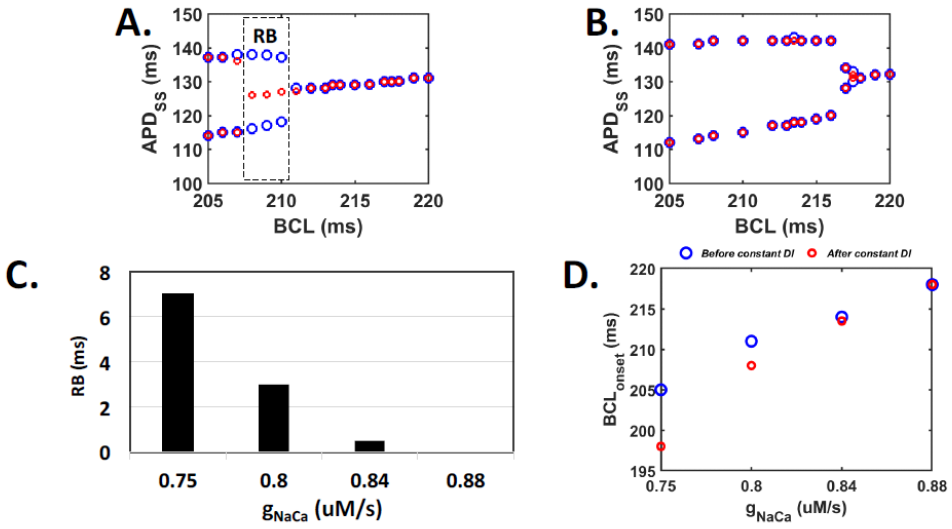

Figure 4.6 Effect of coupling strength on Region of bistability: Overlap of bifurcation diagrams from hybrid pacing: constant-BCL pacing at BCL_1 before (blue) and after (red) constant-DI pacing for A) strong V-Ca coupling and B) weak V-Ca coupling. RB is indicated by dashed box in A. C) RB as a function of different V-Ca coupling strengths. D) The shift of BCL_{onset} before (blue) and after (red) constant-DI pacing for varying V-Ca coupling strengths.

4.4 Reversibility of bistable response is variable:

Finally, we investigated if the RB triggered by constant-DI pacing can be reversed by perturbing the system. To achieve this, we applied the hybrid protocol with perturbation (BCL_1 → DI_{const} → BCL_2 → BCL_1). In Figure 4.7, ΔAPD (APD_{SS} – APD_{long} and APD_{SS} – APD_{short}) is plotted as a function of the magnitude of perturbation, δ, for representative BCLs chosen from the RB for normal (blue) and strong V-Ca coupling (red) (BCL_1 = 213.5 ms and BCL_1 = 209 ms respectively). Note that a RB did not exist for weak V-Ca coupling,

and therefore was not plotted. Changes in the cell dynamics were reversed (i.e. the cell returned to alternans) when the magnitude of δ reached a critical value (δcrit), see Table III. The inset in Figure 4.7 further indicates that the transition from a 1:1 response to alternans is qualitatively different for different V-Ca coupling strengths: normal V-Ca coupling resulted in a gradual increase in ΔAPD close to BCL_{onset} before a sharp increase in ΔAPD resulting in alternans while strong V-Ca coupling abruptly transitioned into alternans.

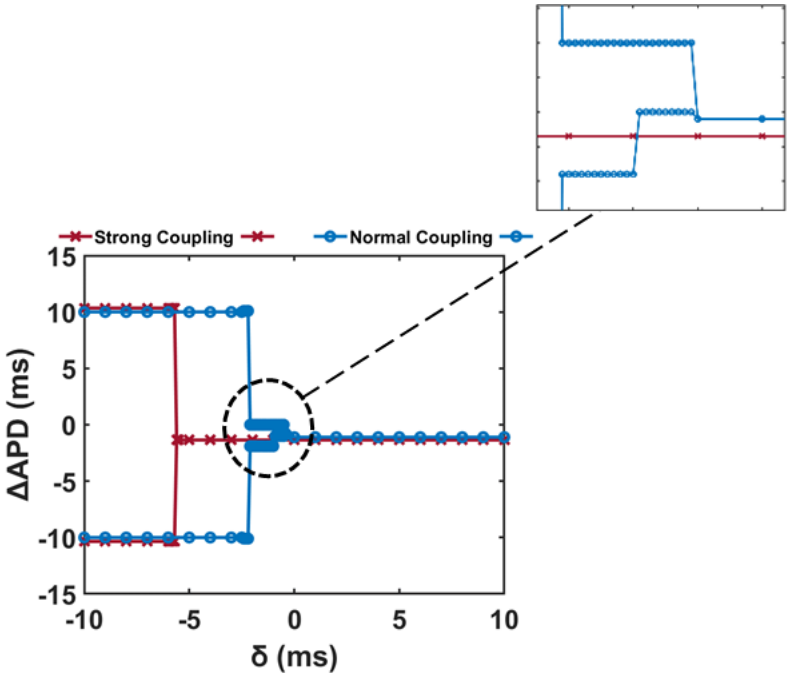

Figure 4.7 Changes in bistability in response to perturbation: The magnitude of alternans ΔAPD as a function of δ when the hybrid pacing protocol with perturbation was applied for the case of strong (red) and normal (blue) V-Ca coupling.

In Figure 4.8, the reversibility of the dynamic responses is explored for different BCL_1 within the RB from Figure 4.6 A. For this analysis, three BCL_1 (208, 209 and 210 ms) were chosen from within the RB for strong V-Ca coupling in Figure 4.6 A. Figure 4.8 A demonstrates three overlapping bifurcation diagrams for the BCL_1, and Figure 4.8 B demonstrates ΔAPD as a function of δ. Moving BCL_1 closer to BCL_{onset} (211 ms) resulted in the δcrit increasing from 3.6 ms (BCL = 208 ms) to 5.5 ms (BCL = 209 ms). At BCL = 210 ms, the system did not exhibit alternans (green) for any value of δ. Also, the sharpness in transition to alternans increased as BCL_1 moved closer to BCL_{onset} (comparing yellow and red traces).

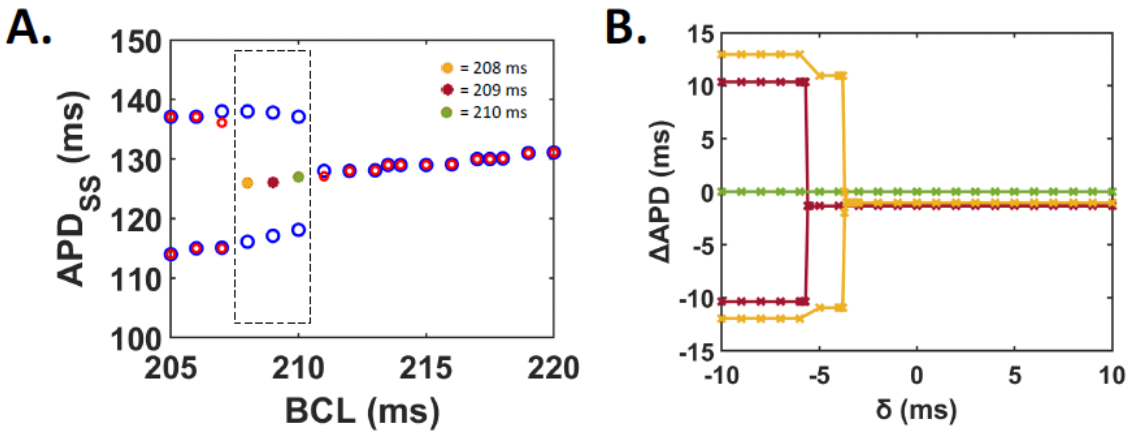

Figure 4.8 Effect of coupling strength on reversibility of bistability: A) Overlap of bifurcation diagrams from three BCL_1 within RB from Fig. 4.6 A (Table 4.3) during hybrid pacing protocol under strong V-Ca coupling. B) The magnitude of alternans ΔAPD as a function of δ for each BCL_1 listed in Table 4.3.

BCL (ms)	δ_{crit} (ms)	ΔAPD (ms)
208	-3.6	24.9
209	-5.5	20
210	-	0

Table 4.3 δ_{crit} required for the system to exhibit alternans after application of constant-DI pacing during strong V-Ca coupling

4.5 Discussion and Future Scope

In this study, we have reiterated that constant-DI pacing suppresses voltage-driven alternans (Cherry, 2017; Kulkarni et al., 2018; Zlochiver et al., 2017). Our main conclusions on investigating the corresponding mechanism are as listed. 1) We discovered that constant-DI pacing introduces bistability in the model and varying V-Ca coupling strength affects the region of bistability. The bistability effect of constant-DI pacing becomes more prominent at stronger coupling strengths and is diminished at weaker coupling strengths. 2) We have also noticed that the reversibility of bistable response varies with the coupling strength, the magnitude of perturbations and the distance of region with respect to BCL_{onset}. It is seen that the absolute value of deviation required for reversibility increases with increasing coupling strength. The robustness of bistability due to constant-DI pacing increases as we move towards regions closer to BCL_{onset}. 3) It must be noted that there exists a region in the neighborhood of bifurcation,

under strong coupling condition, where constant DI permanently remodels the cell and eliminates APD-alternans.

An RB has not previously been observed in cardiac tissue under constant-DI pacing. This new finding suggests constant-DI pacing could affect the dynamics of cardiac tissue in an anti-alternans manner and encourages future research into constant-DI pacing. Moreover, the RB was altered through changes in V-Ca coupling allowing for potentially further anti-alternans benefits.

Although past studies (Jordan & Christini, 2004b; Kihara & Morgan, 1991; McIntyre et al., 2014) have concluded that DI-dependent restitution of APD is not necessary for alternans of APD to occur, they concur that restitution does contribute to alternans and the modification of diastolic interval to minimize alternans can possibly decrease the contribution from one component generating alternans. It needs to be noted that constant-DI pacing has successfully suppressed the formation of repolarization alternans in 2D models within the physiological range of heart rates (Zlochiver et al., 2017). However, at higher activation rates and spatially complex studies have noted constant-DI pacing may not eliminate alternans. In the past, the mechanism of alternans persistence under constant-DI condition has been explained by combining memory dynamics with calcium cycling. This proves that there is a pressing need to analyze the response to constant-DI pacing in conjunction with various interrelated cellular dynamics. In our study, we have shown that it is worthwhile to explore the mechanism of constant-DI effects in correlation with the V-Ca coupling strength.

It is well known that alternative changes in the amount of calcium released from the SR are likely to be the primary cause of mechanical alternans and the change in these transients could be due to the effects of alteration in membrane properties such as the

diastolic interval. Through the results of this study, we might be able to extend that constant-DI pacing can constructively alter Ca concentrations briefly which allows the state of 1:1 rhythm to persist even after the condition of a constant diastolic interval is removed. However, there is a trade-off since this mechanism compensates for APD adaptation through stronger fluctuations in calcium transients which could lead to premature calcium alternans.

Previous studies have shown that the coupling between voltage and calcium can lead to unstable voltage dynamics under preserved APD restitution (Kihara & Morgan, 1991; Walker & Rosenbaum, 2003b). In our study, we explore the possibility of the converse hypothesis where V-Ca coupling is used to stabilize alternating APD. In theory, under the condition of strong coupling, the sodium-calcium exchanger is highly activated. Hence, the extrusion of calcium under rapid pacing becomes easier. This facilitates APD adaptation and elimination of alternans at rapid rates. This would explain why the onset of alternans gets pushed farther with increased coupling strengths. The same mechanism might enable the persistence of normal rhythm for a longer period under a strong coupling condition.

Some limitations of our study need to be regarded. Our analysis was conducted on numerical simulations. Hence, the results need to be validated in experimental models. And the experimental implementation of constant-DI pacing remains to be a challenge. We study the effects on a single cell model. The dynamics may vary in tissue models due to cell coupling, conduction velocity restitution, and other higher-order tissue capacities. Further, our findings are limited to the rabbit ventricle model and we have not extended the results to other models. A different intracellular calcium cycling submodel might lead to different responses to V-Ca changes. Our formulation of V-Ca coupling dynamics is single-faceted and grossly simplifies the real physiological situation of the complex

interplay of Ca currents. Also, we have not analyzed the consequence of our analysis on various other calcium-sensitive ionic currents (such as Ca-sensitive Cl- and K+ currents). However, the nature of action potentials under all tested coupling strengths reflected physiologic morphology validating the relevance of our findings.

Future researchers should investigate Ca alternans in the presence of varying V-Ca coupling strengths. In this study, we do not delve deeper into the Ca alternans since we're primarily concerned about the mechanism of suppressing voltage alternans. However, it has been established that the restitution of the Ca transient is independently influenced by other factors besides the DI. We have also shown that increasing coupling strength could lead to premature calcium alternans as a compensation to APD adaptation. Hence, the possibility of calcium alternans under cases of monotonic APD restitution and consequence of V-Ca coupling changes on these Ca alternans need to be pursued in future studies. A detailed analysis of the nature of bifurcation under different coupling strengths need to be conducted. Type association (smooth vs. border collision bifurcation) with coupling related changes could open new avenues to understanding alternans propagation.

We reinstate that cellular alternans has been proven to be the basis of T-wave alternans which is clinically associated with ventricular fibrillation. Further, instabilities in the calcium cycle have shown to aggravate ventricular tachycardia into fibrillation. Hence, the importance of pacing strategies to eliminate alternans is paramount and the exploration of such techniques need to account for interconnected voltage and calcium dynamics. Our study proves that the intricate balance between constant-DI pacing and V-Ca coupling has the potential to permanently remodel the cardiac cell. Future studies in this direction will provide better insight into alternans suppression.

CHAPTER 4: CONCLUSION

In this study, we examined the effect of constant-DI pacing on cardiac cell dynamics. As elaborated in the literature review, the potential of constant-DI pacing to eliminate alternans has been established. However, there is a gap in understanding the cellular mechanisms that mediate these effects. Hence, this study focused on exploring the niche mechanisms that regulate the effects of constant-DI pacing on single ventricular cell. Further, our central claim was that the interplay of voltage and calcium dynamics play an important role in the consequences of constant-DI pacing.

For achieving the central hypothesis, we designed a hybrid pacing protocol with the capability to switch between constant-BCL and constant-DI pacing. We compared the state of the system before and immediately after the constant-DI pacing sequence. This pacing model allowed us to visualize transition in cellular dynamics at a higher temporal resolution. We then introduced short perturbations during the transition following constant-DI pacing to briefly disturb the condition and test the robustness of the induced changes.

We show that in a region close to the bifurcation point constant-DI pacing remodels the cardiac cell. In the absence of perturbations in this region, the cell does not revert to alternans even after the constant-DI condition is removed. This proves that maintaining a constant diastolic interval has altered the dynamics of the cardiac cell enabling it to maintain stable 1:1 rhythm. Increasing the V-Ca coupling strength increases the size of this region. This clearly indicates that the interplay between intracellular calcium-cycle and voltage-dynamics are tightly regulated by the conformation of various calcium channels in the heart and they could impact the cellular effects of constant-DI pacing. And finally, at higher coupling strengths the changes in APD are irreversible despite large

perturbations. That is, beyond a threshold the anti-alternans effect of constant-DI pacing can be made permanent by modulating V-Ca dynamics.

Novelty: Our analysis concluded that maintenance of constant-DI condition can remodel the cardiac cell permanently through its interaction with V-Ca coupling strength and create a region of bistability. These results have never been demonstrated before. Previous findings indicated that suppression of alternans through constant-DI pacing is limited. However, our study uncovered the possibility to modify the effects of constant-DI pacing by altering V-Ca coupling strength and amplifying the benefits henceforth.

Limitations: Our study is limited to single-cell analysis and confined changes to V-Ca coupling since we alter only the sodium-calcium exchanger activity. Also, our model is limited to the rabbit ventricular cell which impedes its translatability across species which have distinct calcium dynamics.

Scope: Future research should consider investigating invasive changes to the intracellular calcium cycle by exploring changes to other calcium transporters and expand the analysis to tissue level studies across various species. Regardless, our results emphasize that the interaction between constant DI condition and calcium cycling can provide better insight into alternans propagation and elimination.

REFERENCES:

1. Bauer, S., Röder, G., & Bär, M. (2007). Alternans and the influence of ionic channel modifications: Cardiac three-dimensional simulations and one-dimensional numerical bifurcation analysis. *Chaos (Woodbury, N.Y.)*, *17*(1), 015104. https://doi.org/10.1063/1.2715668
2. Cherry, E. M. (2017). Distinguishing mechanisms for alternans in cardiac cells using constant-diastolic-interval pacing. *Chaos*, *27*(9). https://doi.org/10.1063/1.4999354
3. Cherry, E. M., & Fenton, F. H. (2004). Electrotonic , Memory , and Conduction Velocity Restitution Effects. *American Journal of Physiology. Heart and Circulatory Physiology*, *286*, H2332–H2341.
4. Christini, D. J., Riccio, M. L., Culianu, C. A., Fox, J. J., Karma, A., & Gilmour, R. F. (2006). *Control of Electrical Alternans in Canine Cardiac Purkinje Fibers*. https://doi.org/10.1103/PhysRevLett.96.104101
5. Chudin, E., Goldhaber, J., Garfinkel, A., Weiss, J., & Kogan, B. (1999). Intracellular Ca(2+) dynamics and the stability of ventricular tachycardia. *Biophysical Journal*, *77*(6), 2930–2941. https://doi.org/10.1016/S0006-3495(99)77126-2
6. Cram, A. R., Rao, H. M., & Tolkacheva, E. G. (2011). Toward prediction of the local onset of alternans in the heart. *Biophysical Journal*, *100*(4), 868–874. https://doi.org/10.1016/j.bpj.2011.01.009
7. Dunn, A. M., Hofmann, O. S., Waters, B., & Witchel, E. (2011). Cloaking malware with the trusted platform module. *Proceedings of the 20th USENIX Security Symposium*, pp. 395–410.
8. Euler, D. E. (1999). Cardiac alternans: Mechanisms and pathophysiological significance. *Cardiovascular Research*, *42*(3), 583–590. https://doi.org/10.1016/S0008-6363(99)00011-5
9. Guevara, M. R., Ward, G., Shrier, A., & Glass, L. (1984). Electrical Alternans and Peiod Doubling Bifurcations. *IEEE Computers in CardiologyComputers in Cardiology*, *562*, 167.
10. Hayashi, H., Shiferaw, Y., Sato, D., Nihei, M., Lin, S. F., Chen, P. S., … Qu, Z. (2007). Dynamic origin of spatially discordant alternans in cardiac tissue. *Biophysical Journal*, *92*(2), 448–460. https://doi.org/10.1529/biophysj.106.091009

11. Jordan, P. N., & Christini, D. J. (2004). Adaptive diastolic interval control of cardiac action potential duration alternans. *Journal of Cardiovascular Electrophysiology*. https://doi.org/10.1046/j.1540-8167.2004.04098.x
12. Kakade, V., Zhao, X., & Tolkacheva, E. G. (2013). Using dominant eigenvalue analysis to predict formation of alternans in the heart. *Physical Review E - Statistical, Nonlinear, and Soft Matter Physics*, *88*(5), 1–7. https://doi.org/10.1103/PhysRevE.88.052716
13. Kanu, U. B., Iravanian, S., Gilmour, R. F., & Christini, D. J. (2011). Control of action potential duration alternans in canine cardiac ventricular tissue. *IEEE Transactions on Biomedical Engineering*, *58*(4), 894–904. https://doi.org/10.1109/TBME.2010.2089984
14. Karma, A. (1994). Electrical alternans and spiral wave breakup in cardiac tissue. *Chaos*, *4*(3), 461–472. https://doi.org/10.1063/1.166024
15. Kihara, Y., & Morgan, J. P. (1991). Abnormal Cai2+ handling is the primary cause of mechanical alternans: study in ferret ventricular muscles. *The American Journal of Physiology*, *261*(6 Pt 2), H1746-55. https://doi.org/10.1152/ajpheart.1991.261.6.H1746
16. Kitajima, H., & Yazawa, T. (2011). *Modified Luo-Rudy model and its bifurcation analysis for suppressing alternans*. (1), 390–394.
17. Kulkarni, K., Lee, S. W., Kluck, R., & Tolkacheva, E. G. (2018). Real-Time Closed Loop Diastolic Interval Control Prevents Cardiac Alternans in Isolated Whole Rabbit Hearts. *Annals of Biomedical Engineering*, *46*(4), 555–566. https://doi.org/10.1007/s10439-018-1981-2
18. Kulkarni, K., Visweswaran, R., Zhao, X., & Tolkacheva, E. G. (2015). Characterizing Spatial Dynamics of Bifurcation to Alternans in Isolated Whole Rabbit Hearts Based on Alternate Pacing. *BioMed Research International*, *2015*. https://doi.org/10.1155/2015/170768
19. Mahajan, A., Shiferaw, Y., Sato, D., Baher, A., Olcese, R., Xie, L.-H., … Weiss, J. N. (2008). A rabbit ventricular action potential model replicating cardiac dynamics at rapid heart rates. *Biophysical Journal*, *94*(2), 392–410. https://doi.org/10.1529/biophysj.106.98160
20. McIntyre, S. D., Kakade, V., Mori, Y., & Tolkacheva, E. G. (2014). Heart rate variability and alternans formation in the heart: The role of feedback in cardiac

dynamics. *Journal of Theoretical Biology*. https://doi.org/10.1016/j.jtbi.2014.02.015

21. McIntyre, S. D., Mori, Y., & Tolkacheva, E. G. (2011). Local onset of voltage and calcium alternans in the heart. *ASME 2011 Dynamic Systems and Control Conference and Bath/ASME Symposium on Fluid Power and Motion Control, DSCC 2011*, *2*, 607–610. https://doi.org/10.1115/DSCC2011-6148
22. McIntyre, S. D., Kakade, V., Mori, Y., & Tolkacheva, E. G. (2014). Heart rate variability and alternans formation in the heart: The role of feedback in cardiac dynamics. *Journal of Theoretical Biology*, *350*, 90–97. https://doi.org/10.1016/j.jtbi.2014.02.015
23. Mulpuru, S. K., Madhavan, M., McLeod, C. J., Cha, Y. M., & Friedman, P. A. (2017). Cardiac Pacemakers: Function, Troubleshooting, and Management: Part 1 of a 2-Part Series. *Journal of the American College of Cardiology*, *69*(2), 189–210. https://doi.org/10.1016/j.jacc.2016.10.061
24. Narayan, S. M. (2006). T-wave alternans and the susceptibility to ventricular arrhythmias. *Journal of the American College of Cardiology*. https://doi.org/10.1016/j.jacc.2005.08.066
25. Nolasco, J. B., & Dahlen, R. W. (2017). A graphic method for the study of alternation in cardiac action potentials. *Journal of Applied Physiology*, *25*(2), 191–196. https://doi.org/10.1152/jappl.1968.25.2.191
26. Nolasco, J. B., & Dahlen, R. W. (1968). A graphic method for the study of alternation in cardiac action potentials. *Journal of Applied Physiology*, *25*(2), 191–196. https://doi.org/10.1152/jappl.1968.25.2.191
27. Otani, N. F. (2017). Theory of the development of alternans in the heart during controlled diastolic interval pacing. *Chaos*. https://doi.org/10.1063/1.5003250
28. Pastore, J. M., Girouard, S. D., Laurita, K. R., Akar, F. G., & Rosenbaum, D. S. (1999). *Mechanism Linking T-Wave Alternans to the Genesis of Cardiac Fibrillation*. Retrieved from http://www.circulationaha.org
29. Rosell, R., Gomez-Codina, J., Camps, C., Maestre, J. A., Padille, J., Cantó, A., … Abad, A. (1994). The New England Journal of Medicine Downloaded from nejm.org at NovartisLibrary on November 11, 2013. For personal use only. No other uses without permission. Copyright © 1994 Massachusetts Medical Society. All rights reserved. *The New England Journal of Medicine*, *330*(3), 153–158.

30. Shiferaw, Y., Watanabe, M. A., Garfinkel, A., Weiss, J. N., & Karma, A. (2003). Model of Intracellular Calcium Cycling in Ventricular Myocytes. In *Biophysical Journal* (Vol. 85).
31. Tolkacheva, E. G., Romeo, M. M., Guerraty, M., & Gauthier, D. J. (2004). Condition for alternans and its control in a two-dimensional mapping model of paced cardiac dynamics. *Physical Review E - Statistical, Nonlinear, and Soft Matter Physics*, *69*(3 1), 1–8. https://doi.org/10.1103/PhysRevE.69.031904
32. Tolkacheva, E. G., & Visweswaran, R. (2013). Spatio-temporal evolution and prediction of action potential duration and calcium alternans in the heart. *Cardiovascular Disease*.
33. Verrier, R. L., & Malik, M. (2013). Electrophysiology of T-wave alternans: Mechanisms and pharmacologic influences. *Journal of Electrocardiology*, *46*(6), 580–584. https://doi.org/10.1016/j.jelectrocard.2013.07.003
34. Virani, S. S., Alonso, A., Benjamin, E. J., Bittencourt, M. S., Callaway, C. W., Carson, A. P., … Heard, D. G. (2020). Heart disease and stroke statistics—2020 update: A report from the American Heart Association. In *Circulation*. https://doi.org/10.1161/CIR.0000000000000757
35. Walker, M. L., & Rosenbaum, D. S. (2003). Repolarization alternans: Implications for the mechanism and prevention of sudden cardiac death. *Cardiovascular Research*. https://doi.org/10.1016/S0008-6363(02)00737-X
36. Ward, G., Shrier, A., & Glass, L. (1984). *Street, 300*.
37. Watanabe, M. A., Fenton, F. H., Evans, S. J., Hastings, H. M., & Karma, A. (2001). Mechanisms for discordant alternans. *Journal of Cardiovascular Electrophysiology*. https://doi.org/10.1046/j.1540-8167.2001.00196.x
38. Wu, R., & Patwardhan, A. (2006). Mechanism of repolarization alternans has restitution of action potential duration dependent and independent components. *Journal of Cardiovascular Electrophysiology*, *17*(1), 87–93. https://doi.org/10.1111/j.1540-8167.2005.00319.x
39. Zlochiver, S., Johnson, C., & Tolkacheva, E. G. (2017). Constant DI pacing suppresses cardiac alternans formation in numerical cable models ARTICLES YOU MAY BE INTERESTED IN. *Chaos*, *27*, 93903. https://doi.org/10.1063/1.4999355

40. Echebarria, B., & Karma, A. (2002). Spatiotemporal control of cardiac alternans. *Chaos*, *12*(3), 923–930. https://doi.org/10.1063/1.1501544

APPENDIX

The sodium calcium exchanger current is defined by the Hund-Rudy model using the following equation. All parameter used are defined in Table. A.1

$$I_{Naca} = g_{NaCa} * \frac{1}{\mathrm{K_{m;Na}^3} + \mathrm{Na_o^3}} * \frac{1}{\mathrm{K_{m;Ca}} + \mathrm{Ca_o}} * \frac{\mathrm{e^{\varepsilon a} Na_i^3 Ca_o} - \mathrm{e^{(\varepsilon-1)a} Na_o^3 c_s}}{1 + \mathrm{k_{sat} e^{(\varepsilon-1)a}}}$$

Parameter	Definition	Value
Na_o	External sodium concentration	140 mM
Ca_o	External calcium concentration	1.8 mM
Na_i	Internal sodium concentration	14 mM
$K_{m,Na}$	Luo-Rudy II constant	87.5 mM
$K_{m,Ca}$	Luo-Rudy II constant	1.38 mM
K_{sat}	Luo-Rudy II constant	0.1
ε	Luo-Rudy II constant	0.35

c_s	Average submembrane free calcium concentration	0.32 uM

Table A.1 Hund-Rudy model for Sodium-Calcium exchanger current

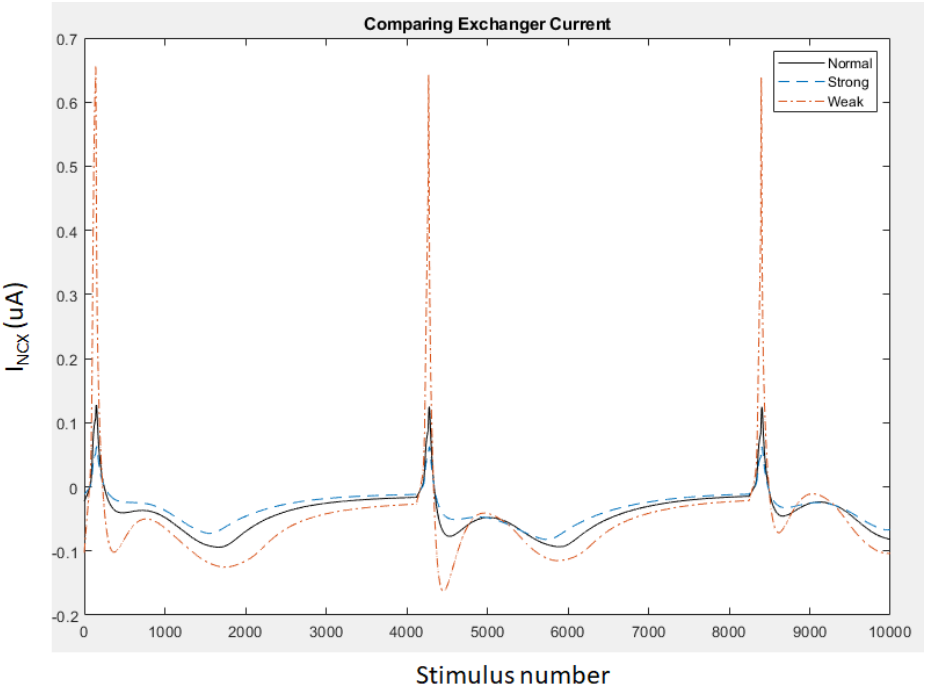

Figure A.1 Sodium-calcium exchanger current: Effect of V-Ca coupling strength on sodium-calcium exchanger current dynamics. Increase in coupling strength (blue) tightly regulates I_{NCX} while weak coupling strength (orange) leads to greater swing in both inward and outward currents leading to unstable dynamics.

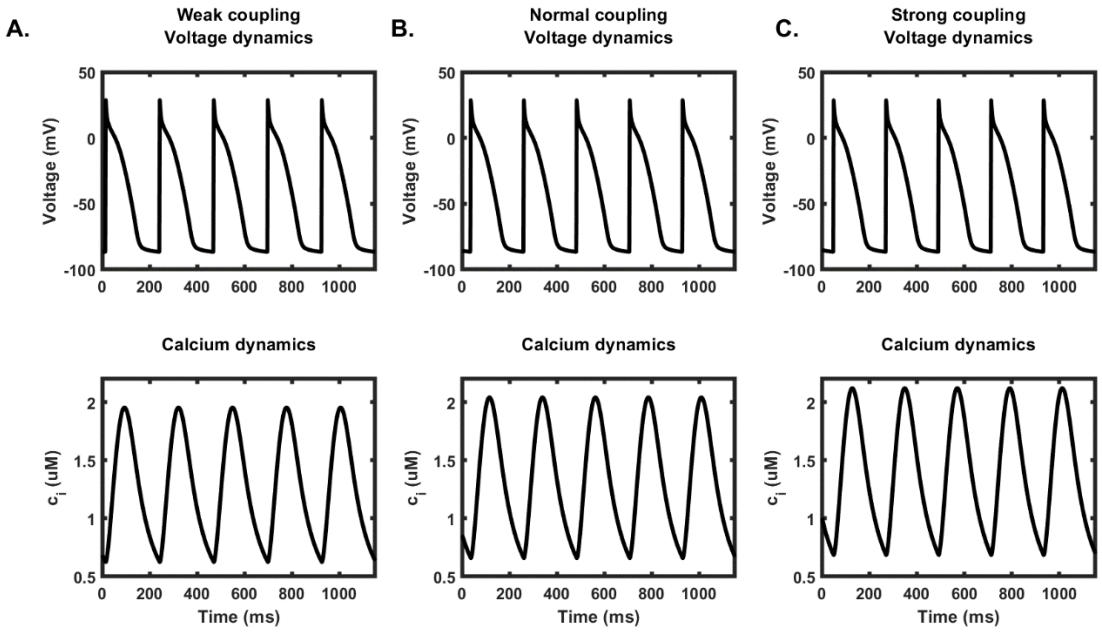

Figure A.2 Changes in voltage and calcium dynamics with coupling strength (normal rhythm) The rabbit cell was paced at a constant BCL = BCL_{onset} + 10ms (no alternans region) and the corresponding APD duration and calcium transient peak was compared between the different coupling strengths. A) Weak coupling (BCL = 227 ms) B) Normal coupling (BCL = 223.5 ms) C) Strong coupling (BCL = 221 ms). The APD duration and amplitude of calcium transient are summarized in Table. A.2

Coupling strength	**Weak**	**Normal**	**Strong**
g_{NaCa} (uM/s)	0.88	0.84	0.80
APD (ms)	123	121	119
Ci (uM)	1.32	1.38	1.43

Table A.2 APD and calcium-transient amplitude with varying coupling strengths